Phase of atmospheric secondary organic material affects its reactivity

Mikinori Kuwata and Scot T. Martin[1]

School of Engineering and Applied Sciences and Department of Earth and Planetary Sciences, Harvard University, Cambridge, MA 02138

Edited by Mark H. Thiemens, University of California San Diego, La Jolla, CA, and approved September 11, 2012 (received for review May 29, 2012)

The interconversion of atmospheric organic particles among solid, semisolid, and liquid phases is of keen current scientific interest, especially for particles of secondary organic material (SOM). Herein, the influence of phase on ammonia uptake and subsequent particle-phase reactions was investigated for aerosol particles of adipic acid and α-pinene ozonolysis SOM. The nitrogen content of the particles was monitored by online mass spectrometry for increasing ammonia exposure. Solid and semisolid adipic acid particles were inert to the ammonia uptake for low RH (<5%). For the solid particles, ammonia exposure at high relative humidity (RH; >94%) induced a first-order deliquescence phase transition into aqueous particles. Solid particles exposed to supersaturated (RH >100%) conditions and cycled back to high RH (>94%), thereby becoming acidic metastable particles, underwent a gradual second-order transition upon ammonia exposure to form aqueous, partially neutralized particles. For α-pinene SOM, ammonia exposure at low RH increased the particle-phase ammonium content by a small amount. Mass spectrometric observations suggest a mechanism of neutralization and co-condensation of acidic gas-phase species, consistent with a highly viscous semisolid upon which adsorption occurs. At high RH the ammonium content increased greatly, indicative of rapid diffusion and absorption in a liquid environment. The mass spectra indicated the production of organonitrogen compounds, possibly by particle-phase reactive chemistry. The present results demonstrate that phase can be a key regulator of the reactivity of atmospheric SOM particles.

atmospheric chemistry | chemical aging | organic aerosol | collection efficiency

The production, transformation, and removal processes of atmospheric organic aerosol particles have been intensively investigated in recent years, as motivated in large part by their important roles in climate regulation and air quality (1). A significant portion of the mass concentration of atmospheric particles is produced by the oxidation of biogenic and anthropogenic volatile organic compounds to form low-volatility products. These products in the particle phase are referred to as secondary organic material (SOM). Present models assume that semivolatile condensable species are in equilibrium between the particle and gas phases (2–6). These models further assume a low-viscosity liquid particle phase so that diffusion is rapid, and for these circumstances the thermodynamic activities of absorbed molecules are homogeneous throughout the particle (3). Recent studies, however, have demonstrated that SOM particles for some reaction conditions can also exhibit the physical properties of a solid (7–10). For instance, at low to intermediate relative humidity (RH) at 25 °C, some SOM particles bounced from smooth, hard surfaces, a behavior that was not observed for liquid particles (8, 11). Furthermore, for some SOM particles the kinetics of evaporation were not consistent with liquid particles (9). These findings pointing in the direction of nonliquid SOM particles under some conditions imply that their viscosity is sufficiently high to maintain solid-like properties, although they do not have ordered crystalline structures (12). The SOM might be described as a semisolid, characterized by a dynamic viscosity η of $10^2 < \eta < 10^{12}$ Pa s (12–15). Liquids have lower values ($\eta < 10^2$ Pa s).

The atmospheric occurrence of organic semisolid particles can have important implications for aging processes. Aging can significantly alter a particle's physicochemical properties, including hygroscopic and optical properties (1). Diffusion of molecules in a semisolid, however, is much slower than in a liquid. The Stokes–Einstein equation states that the diffusion coefficient D is proportional to η^{-1} (12). The timescale for homogeneous mixing by diffusion is on the order of microseconds to milliseconds for liquid submicron particles. By comparison, for semisolid particles the timescale can range from seconds to days, depending on the viscosity of particles (16). Correspondingly, aging processes are slowed considerably and possibly even completely shifted from absorption to adsorption. For instance, these effects occur for the ozonolysis of oleic acid when present in host matrices of variable viscosity (17–19). Oleic acid is a hydrophobic compound associated with primary emissions from meat cooking. By comparison, secondary organic material belongs to a different class of materials. In particular, SOM is composed of highly functionalized branched oxygenated compounds that can be hygroscopic. Water, when present in SOM, can serve both as an important direct reactant as well as an important plasticizer to decrease viscosity and thereby affect diffusivity and overall reaction rates in the particle phase (12). Moreover, SOM is composed of myriad compounds that are produced by chemical reactions both in the gas and particle phases, and SOM characteristics therefore cannot be fully represented by pure compounds, motivating the need to investigate directly the possible phase-dependent chemical reactivity of SOM particles. At present time, however, the roles of SOM phase and viscosity on the uptake of gas-phase species and possible subsequent heterogeneous chemistry have not yet been investigated experimentally, especially in conjunction with the interplay with the effects of water.

Herein, experimental results are presented concerning how the phase of organic particles affects their reactivity. The focus is on the uptake of ammonia by adipic acid and α-pinene ozonolysis secondary organic material. Adipic acid is selected as a simple reference compound because of its property to form various phases, depending on the exposure history to RH (20–22). α-Pinene is chosen because of its atmospheric significance and because α-pinene SOM is solid or semisolid, at least for some experimental conditions (8, 11). α-Pinene SOM can have the physical properties of a solid from 5% RH up to at least 60% RH (limit of conducted measurements), implying that differences in the chemical reactivity of solid and liquid α-pinene SOM can have widespread applicability for atmospheric conditions (11). Ammonia is emitted to the atmosphere both from natural and anthropogenic sources, and its atmospheric concentration is increasing at the present time, in part because of worldwide

Author contributions: M.K. and S.T.M. designed research; M.K. performed research; M.K. analyzed data; and M.K. and S.T.M. wrote the paper.

The authors declare no conflict of interest.

This article is a PNAS Direct Submission.

[1]To whom correspondence should be addressed. E-mail: scot_martin@harvard.edu.

This article contains supporting information online at www.pnas.org/lookup/suppl/doi:10.1073/pnas.1209071109/-/DCSupplemental.

increases in fertilizer use, animal husbandry, and temperature (23–25). In addition to atmospheric importance, the nitrogen atom of ammonia is advantageous for the strategy of the conducted uptake experiments: A particle of otherwise very low nitrogen content is characterized by high-resolution mass spectrometry that is capable of differentiating nitrogen-containing ions. Other reactive compounds such as ozone and hydroxyl radical do not have this feature because they are atomic constituents of the SOM itself (16, 26). The results of the experiments show a strong effect of organic phase on ammonia uptake, including reactive chemistry and the formation of organonitrogen bonds.

Particle Generation and Ammonia Exposure

Adipic acid particles were generated by homogeneous nucleation from a supersaturated vapor under dry conditions (RH <5%). α-Pinene SOM particles were produced using the Harvard Environmental Chamber (HEC) operated under dry conditions without the injection of seed particles. The produced aerosol particles were employed in four different types of experiments in which the RH sequence differed (Fig. 1). These sequences included: (*i*) dry, (*ii*) supersaturated → dried, (*iii*) humidified, and (*iv*) supersaturated (Table 1). After an RH sequence, the particles were exposed to gaseous ammonia for a mean residence time of 400 s. The ammonia concentration X_{NH_3} in the reactor was increased stepwise from 0 to 7.8 ppm during the course of a single experiment. The second stepwise increase to 0.8 ppm NH_3 ensured excess ammonia with respect to the possible acidity of the tested adipic acid and α-pinene SOM aerosols based on their mass concentrations. The mean ammonia exposure (0.8–7.8 ppm · 400 s) of the experiments was on the order of that in the atmosphere for typical ammonia concentrations (1–10 parts per billion) and particle residence times (7–10 d) (27).

After exposure to ammonia and desiccation in a diffusion dryer, particle number–diameter distributions were measured using a scanning mobility particle sizer (SMPS; TSI Inc.) (28). Particle composition was characterized using an aerosol mass spectrometer (AMS; Aerodyne Research Inc.) (29). The AMS quantified the particle-phase organic mass concentration M_{org} and the particle-phase ammonium mass concentration M_{NH_4}. The latter was quantified using the high-resolution signal intensities for the NH^+, NH_2^+, and NH_3^+ ions. The CO_2^+ ion originated in large part from dicarboxylic acids, and the ratio of M_{NH_4} to the intensity of CO_2^+ (m/z, 43.9898), abbreviated hereafter as $M_{CO_2^+}/M_{NH_4}$, served as a metric of the degree of acid neutralization of the particles (30). The collection efficiency (CE) of the AMS was calculated as the ratio of the organic particle mass concentration M_{org} indicated by the AMS to that measured by the SMPS after adjustment for particle density. Low collection efficiencies can occur for solid particles that bounce on the AMS vaporizer (31).

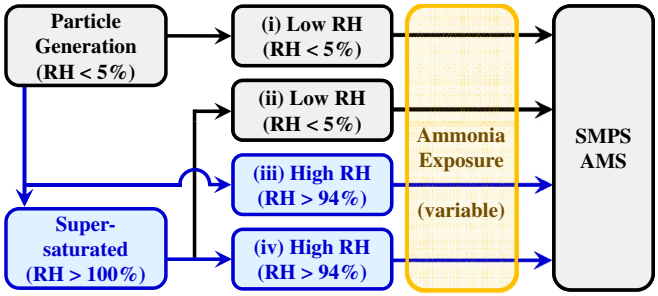

Fig. 1. Schematic diagram of the four different types of experiments labeled *i* through *iv*. The sequence of exposure to RH differs among the experiments (Table 1). The susceptibility of the particles to ammonia uptake is measured by the magnitude of changes in diameter (SMPS) and mass (AMS) upon exposure to variable concentrations of ammonia. Gray background, low RH (<5%); blue background, high RH (>94%) or supersaturated.

Table 1. The sequence of exposure to relative humidity for the four different types of experiments (labeled *i* through *iv*)

Label	Description	RH sequence	RH of ammonia exposure
(*i*)	Dry	<5%	<5%
(*ii*)	Supersaturated → Dried	<5% →> 100% →< 5%	<5%
(*iii*)	Humidified	<5% →> 95%	>94%
(*iv*)	Supersaturated	<5% →> 100% →> 95%	>94%

Adipic Acid

Fig. 2 summarizes the observations of ammonia uptake by adipic acid for the four experiment types *i* to *iv*. Fig. 2*A* shows that the AMS collection efficiency for dry crystalline particles of experiment *i* was stable around 0.15, even for the highest ammonia exposures. For comparison, crystalline ammonium sulfate had a similar collection efficiency (31). Fig. 2*A* also shows that the collection efficiency increased to 0.5 after cycling from supersaturated to dry conditions in experiment *ii*, indicative of a hysteresis effect that resulted in softer particles. Adipic acid deliquesces in supersaturated environments (32), so the inference from the results is that the adipic acid particles did not re-form a crystalline solid at low RH. As in the case of other organic materials, including various dicarboxylic acids (15, 33), adipic acid readily forms a metastable amorphous state, rather than crystallizing, upon desiccation (20, 22, 32, 34).

Compared to the results of Fig. 2*A* that show limited ammonia uptake at low RH, ammonia uptake by adipic acid at high RH (>94%) was considerably different (Fig. 2*B*). The crystalline particles of experiment *iii* retained their phase to high RH, as shown by the low collection efficiency prior to ammonia exposure. This result is consistent with an estimated deliquescence RH of adipic acid of 99.9% for large particles and, because of the Kelvin effect, of over 100% for submicron particles (32, 35). For increasing ammonium exposure, however, an abrupt change to unity collection efficiency occurred ($X_{NH_3} = 1$ ppm). The inference is that a phase transition occurred from solid to liquid. Ammonia induced the deliquescence of the adipic acid. The solubility of ammonium adipate (0.504 kg kg^{-1} H_2O) is nearly 30 times higher than that of adipic acid (0.018 kg kg^{-1} H_2O) (34, 36). Ammonia can dissolve into the water layer on the particle surface and initiate the abrupt dissolution of the adipic acid crystal by the co-uptake of additional water and ammonia (37). The event can be categorized as a first-order phase transition. Changes in particle morphology also confirm a transition from an irregular shape to a sphere, as is typically characteristic of a liquid (Fig. S1).

In comparison, in experiment *iv*, rather than an abrupt transition, the collection efficiency of the metastable particles gradually increased for higher ammonia exposures at high RH, eventually also becoming unity and suggesting fully liquid particles for $X_{NH_3} = 1$ ppm (Fig. 2*B*). The inference is that ammonia dissolved into the metastable material by an absorption mechanism and further enhanced the amount of water, which served as a plasticizer to facilitate the process. This event is categorized as second-order phase transition. The ammonia uptake might have been thermodynamic or kinetically limited during the several stepwise increases of ammonia exposure.

Fig. 2 *C* and *D* shows the particle-phase ammonium content, expressed as M_{NH_4}/M_{org}, for increasing ammonia exposure. For low RH, the crystalline particles did not take up any detectable ammonia, even to the highest value of X_{NH_3} (Fig. 2*C*, *i*). The semisolid particles took up a detectable but low quantity of ammonia (M_{NH_4}/M_{org} of approximately 0.001) (Fig. 2*C*, *ii*). For comparison, direct injection of ammonia into the vaporization/condensation particle generator (i.e., adipic acid was still in the vapor phase) resulted in particles having significantly more ammonia ($M_{NH_4}/M_{org} = 0.02$; Fig. S2). This result suggests that

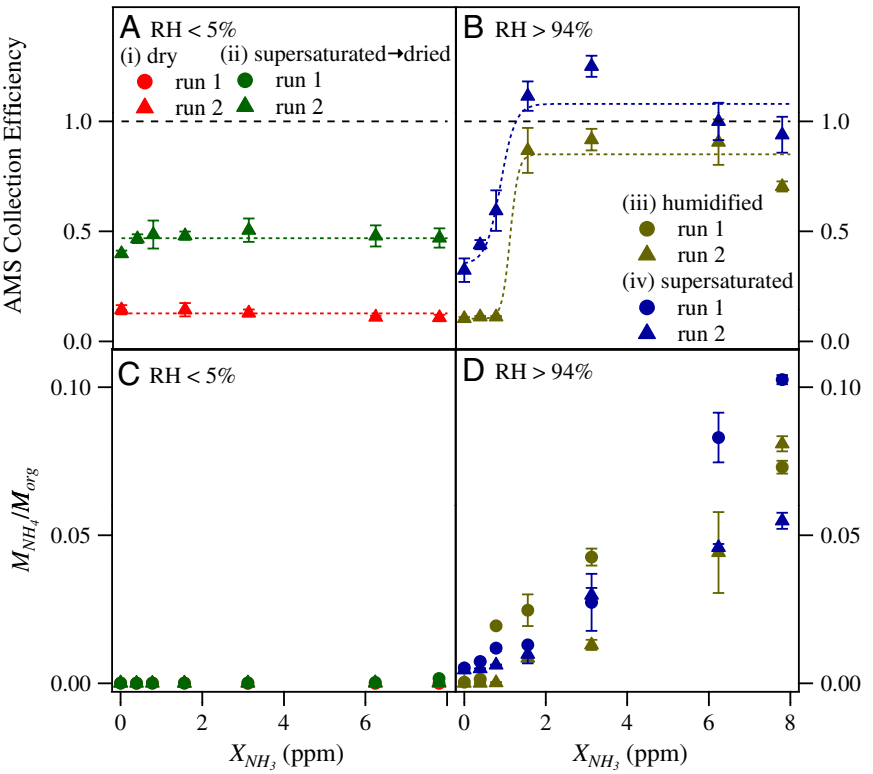

Fig. 2. Ammonia uptake by adipic acid for the four experiment types *i* to *iv*. The error bars in panels *A* through *D* represent one standard deviation for averaging periods of 30 min. (*A* and *B*) AMS collection efficiency for increasing ammonia exposure. Colored dashed lines are drawn to guide the eye. Dashed lines represent no significant particle bounce on the AMS vaporizer and are drawn at unity collection efficiency. Results are shown for replicate runs. For run 1, SMPS data were not recorded, and an AMS collection efficiency is therefore not reported. (*C* and *D*) Particle-phase ammonium content for increasing ammonia exposure. The ammonium content is expressed as the ratio of M_{NH_4} to M_{org}, both measured by the AMS.

ammonia uptake by semisolid and crystalline adipic acid was kinetically rather than thermodynamically limited at low RH.

For high RH (Fig. 2*D*), the crystalline particles did not take up ammonia prior to deliquescence (i.e., experiment *iii* for $X_{NH_3} < 1$ ppm). After the ammonia-induced deliquescence formed a liquid, the particle-phase ammonium content increased continuously for higher values of X_{NH_3}. In comparison to the results for the crystalline phase, the semisolid phase had a non-negligible ammonium content even without any intentional exposure to ammonia (Fig. 2*D*, *iv*). A trace amount of ammonia was present in the purified air. As the ammonia concentration was stepwise increased, the particle-phase ammonium content likewise gradually and monotonically increased. This behavior is consistent with a second-order phase transition whereas the uptake by the crystalline particles is consistent with a first-order phase transition. The magnitude of M_{NH_4}/M_{org} approached 0.1 for the highest values of X_{NH_3}. This value is less than half that of ammonium adipate ($M_{NH_4}/M_{org} = 0.23$), indicating that the particles of experiments *iii* and *iv* were not fully neutralized, even for the highest values of X_{NH_3}.

The results for ammonia uptake by adipic acid can be summarily interpreted, as follows. Crystalline particles at low RH were inert because ammonia did not diffuse through the lattice during the observation period. Semisolid particles at low RH took up small amounts of ammonia even at low RH. A fractional neutralization of 0.001/0.23 took place. This extent of neutralization is consistent with a surface layer (<0.5 nm) for 200- to 400-nm particles, indicating that bulk diffusion was negligible during the observation period. For high RH, by comparison, water absorption acted as a plasticizer that decreased viscosity, increased the diffusion coefficient, and led to extensive ammonia uptake by absorption.

α-Pinene Secondary Organic Material

Fig. 3 summarizes the observations of particle-phase ammonium content of α-pinene SOM for the four experiment types *i* to *iv*. There was an ammonia uptake approximately 10 times greater at high RH (M_{NH_4}/M_{org} of approximately 0.03) compared to low RH (M_{NH_4}/M_{org} of approximately 0.004). The implication of the ammonia-uptake results is that the viscosity of the α-pinene SOM greatly decreased at high RH so that diffusive uptake of ammonia was more rapid. Measurements of the hygroscopic growth factors of α-pinene SOM suggest that there is less than 1% water for low RH and 25–75% water by volume for high RH (38, 39). In addition to the primary effect (with respect to ammonia uptake) of reducing viscosity, the additional water content can also favor the partitioning of additional acids from the gas to the particle

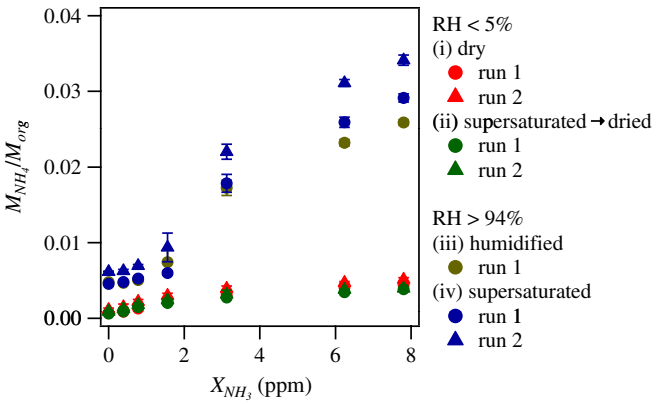

Fig. 3. Ammonia uptake by secondary organic material produced by α-pinene ozonolysis. Results are shown for the four experiment types *i* to *iv*. See also legend for Fig. 2 *C* and *D*.

phase of the aerosol (40, 41). The AMS collection efficiency of the SOM particles was approximately unity at both low and high RH, providing a cautionary note with respect to using bounce for identification of solid phases (i.e., a sufficient but not a necessary condition) (7, 42, 43). The ammonia uptake by α-pinene SOM can also be compared to that of adipic acid at high RH (M_{NH_4}/M_{org} of approximately 0.1) and low RH (M_{NH_4}/M_{org} of approximately 0.001; semisolid branch). Unlike adipic acid, no hysteresis effect between experiments *iii* and *iv* was observed for ammonia uptake by α-pinene SOM. The reversible reactive behavior of α-pinene SOM is in line with reversible physical changes in diameter that are observed for cycles of hydration and dehydration (38, 39).

At low RH, the somewhat increased ammonia uptake of α-pinene SOM relative to adipic acid may be explained by a combination of factors. Both materials retain water to low RH, and the viscosity of α-pinene SOM might be inferred as slightly lower than that of adipic acid, thereby allowing for greater diffusive uptake of ammonia. A second factor, however, is that in the case of α-pinene ozonolysis, many gas-phase molecules are still potentially available for condensation to the particle phase. For α-pinene ozonolysis, Na et al. (44) demonstrated that the injection of gaseous ammonia led to the partitioning of low-volatility ammonium salts of organic acids from the gas phase to the particle phase. This phenomenon can also be a factor that increases M_{NH_4}/M_{org} and could be especially significant at low RH because of the small baseline value of M_{NH_4}/M_{org}. In support of a significant contribution by this pathway, Fig. 4 shows correlation plots between ammonium content (given by M_{NH_4}/M_{org}) and dicarboxylic acid content (given by $M_{CO_2^+}/M_{org}$). The positive monotonic correlation apparent in Fig. 4*A* for low RH is evidence in favor of co-condensation of acids and ammonium in the form of neutralized salts.

For the high-RH experiments, in reverse of the trend at low RH, the α-pinene SOM took up approximately 70% less ammonia than did adipic acid (Fig. 3). Again, this difference can have several contributing factors. For $X_{NH_3} < 1.56$ ppm, small amounts of ammonia uptake occurred, and Fig. 4*B* shows a positive monotonic correlation that again suggests the mechanism of co-condensation of acids and ammonia from the gas phase to the particle phase of the aerosol. For higher concentrations ($X_{NH_3} > 3.1$ ppm), however, the co-condensation curve saturated (Fig. 4*B*), even as ammonia uptake increased greatly (Fig. 3). Absorptive partitioning of ammonia and water into the SOM is implied, and the apparent need to reach a threshold value of X_{NH_3} suggests a second-order phase transition occurred to form an aqueous particle, akin to the similar case described for adipic acid. Under these conditions, the lower uptake of ammonia by α-pinene SOM compared to that by adipic acid can be related to the differences in the total acidity (i.e., much higher in the case of the latter).

Fig. 5 demonstrates that, once in the particle phase, a fraction of the ammonia reacted with organic compounds to form covalent bonds between carbon and nitrogen atoms. The series of ions $C_iH_{2(i+1)}N^+$ was observed in the high-resolution mass spectrum. The signal intensity for CH_4N^+ ($i = 1$) was the largest, with significant intensities up to $i = 6$. The organic nitrogen content is expressed for the ordinate of Fig. 5 as the quotient Σ_i/M_{org} using $\Sigma_i = \Sigma_i M_{C_iH_{2(i+1)}N}$ for $i = 1$ to 6 under the assumptions of uniform relative ionization efficiency and mass-proportional ionization efficiency of the organic fragments in the AMS (45). Analysis shows that organic nitrogen did not contribute significantly to the inorganic ammonium signals (46).

Fig. 5 is a plot of the organic nitrogen content of the particles for increasing inorganic nitrogen content. For low RH, the organic nitrogen content remained negligible for all ammonia exposures and RH histories. For high RH, there was high production of organic nitrogen content, with an apparent maximum for M_{NH_4}/M_{org} of approximately 0.007. The upslope portion (i.e., $M_{NH_4}/M_{org} < 0.007$) is as expected and represents a positive correlation between the extent of organonitrogen bond formation and the concentration of inorganic nitrogen in the particle. The downslope portion (i.e., $M_{NH_4}/M_{org} > 0.007$) is at first less expected but is explained by reference to Fig. 3. The maximum corresponds to the threshold value of X_{NH_3} for the second-order phase transition into an aqueous particle.

The rate of formation of the organonitrogen bonds after this phase transition can slow for any of several reasons. For example, a class of organonitrogen-forming reactions that was previously investigated is the production of imines from carbonyls: $R_1COR_2 + NH_3 \rightarrow R_1C(=NH)R_2 + H_2O$ (47). This reaction is initiated by addition of a proton on the carbonyl oxygen, meaning that acid catalyst is important. Upon hygroscopic growth of forming the aqueous particle, both because of dilution and addition ammonia uptake, the pH of the particles (which is initially acidic because of the carboxylic acid production) can increase such that the acid-catalyzed pathway is turned off.

The summarized findings of this study regarding ammonia uptake by adipic acid and α-pinene secondary organic material are represented in Fig. 6. Semisolid adipic acid and α-pinene SOM have, at most, limited ammonia uptake, which occurs in

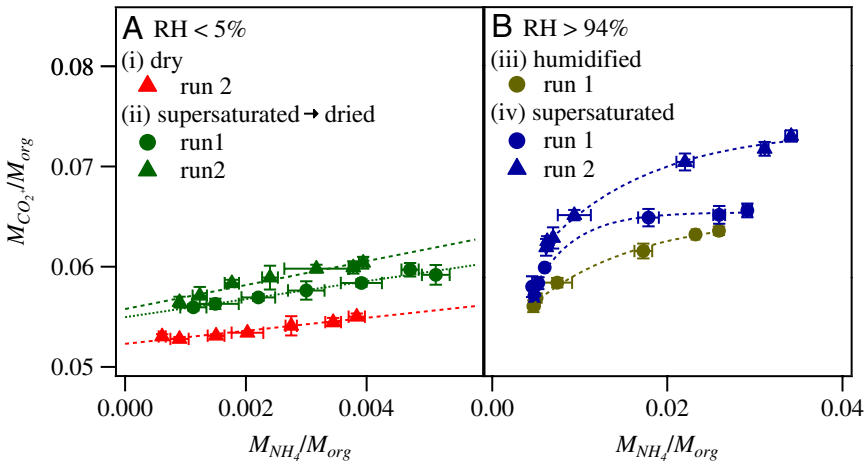

Fig. 4. Correlation plots between ammonium content (given by M_{NH_4}/M_{org}) and carboxylic acid content (given by $M_{CO_2^+}/M_{org}$ under the assumption of uniform relative ionization efficiency in the AMS) for secondary organic material produced by α-pinene ozonolysis. The contribution of gas-phase CO_2 to the CO_2^+ signal intensity was corrected for in the data analysis. (*A* and *B*) Results for the four experiment types *i* to *iv*. Lines are drawn through the data points to guide the eye. Error bars on the data points represent one SD for averaging periods of 30 min. There is a 10-fold increase in ammonium content for the abscissa scale in going from *A* to *B*.

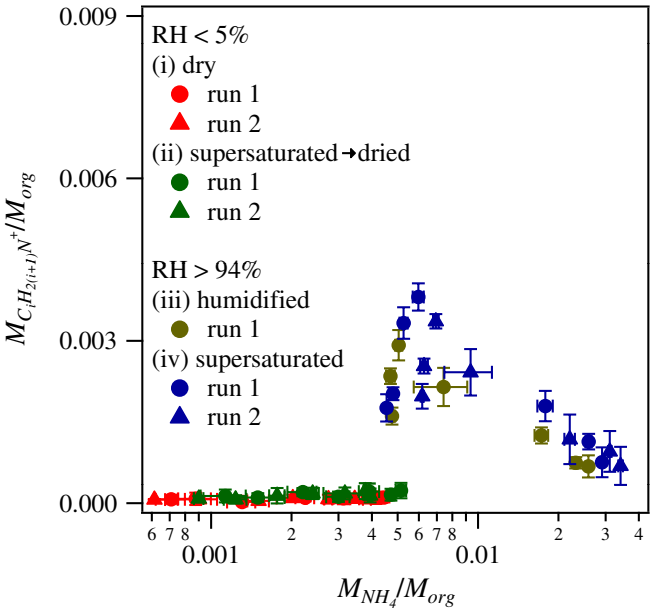

Fig. 5. Relationship between organic nitrogen content and inorganic ammonium content for secondary organic material produced by α-pinene ozonolysis. Results are shown for the four experiment types *i* to *iv*. Error bars on the data points represent one SD for averaging periods of 30 min.

the surface region. After hydration at high RH, however, both adipic acid and α-pinene SOM are highly reactive to ammonia uptake. The implication is that ammonia uptake is thermodynamically favorable but that the rate of uptake can be inhibited by high-viscosity organic material at sufficiently low RH. For α-pinene SOM, the critical value of RH should be above 60%, i.e., the upper limit of the study of Saukko et al. (11) that reported solid properties.

The critical value of RH >60% is within the RH window typical of the diel cycles of the atmospheric boundary layer, meaning that interconversion among solid, semisolid, and liquid phases could therefore be possible on a daily basis and could affect the reaction rates and properties of atmospheric SOM particles by modulating the mass transfer rate of many reactive molecules (8). The present study's results also suggest that organonitrogen bond formation is favored for intermediate particle-phase water content, representing a balance between an acidic environment associated with low water content and a fluid environment induced by high water content. Phase might therefore have an important role in determining the climatic impacts of atmospheric SOM particles by regulating the formation of light-absorbing organonitrogen chromophores (47). Further studies to confirm and generalize the present findings to a range of additional atmospheric contexts are needed, and these studies should include additional types of secondary organic material, such as from isoprene and other terpenes and sesquiterpenes, both by ozonolysis and photooxidation, because the properties of semisolid particles can strongly depend on reaction conditions that influence molecular weight, hygroscopicity, and oxidation state of the SOM (12). Furthermore, the effects of co-present inorganic compounds, such as ammonium nitrate and ammonium sulfate, on SOM phase and reactivity need to be investigated (39). Some of these studies might be successfully conducted in a field context by use of isotopically labeled ammonia, because these molecules would be distinctly detected even in the presence of ambient particle-phase ammonium.

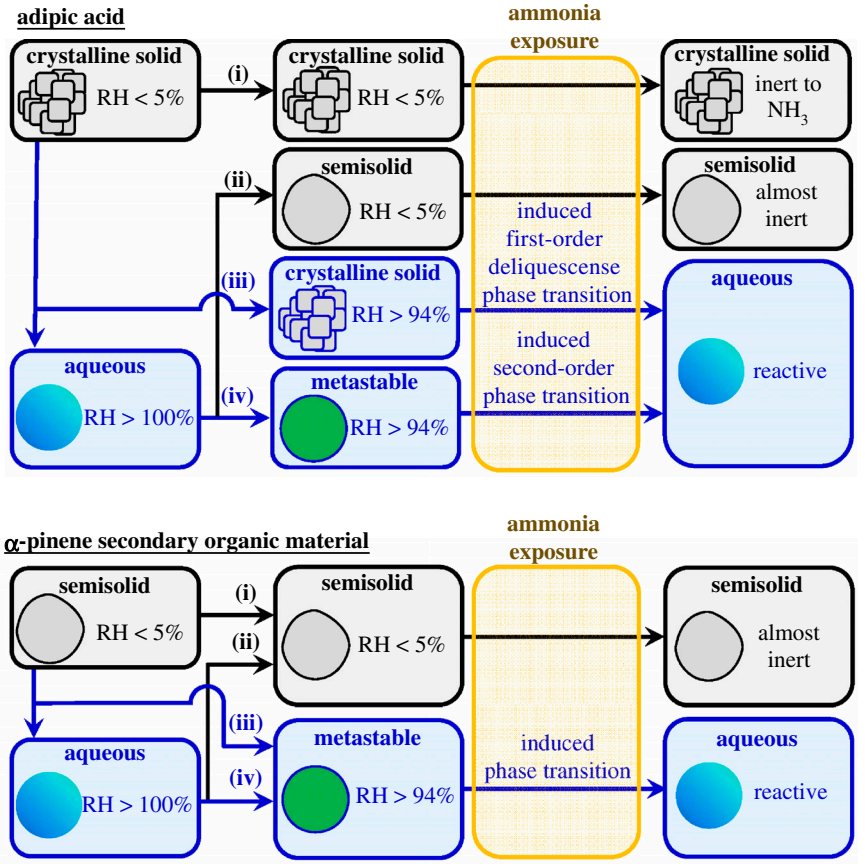

Fig. 6. Cartoon summarizing how the phase of organic particles affects their reactivity. Ammonia uptake is a surrogate for a broad class of reactive and nonreactive uptake processes that occur in the atmosphere and can affect the composition and properties of aerosol particles.

Materials and Methods

Adipic acid particles were produced by homogeneous nucleation of the heated vapor (Fig. S3). Particles of secondary organic material were produced by the dark ozonolysis of α-pinene in the HEC (42, 48). The HEC was operated as a continuously mixed flow reactor. Purified air produced by a zero air generator (AADCO-737) at <5% RH was employed. No seed particles were injected. Particles in the HEC outflow were analyzed.

The phase of the particles was regulated by use of one of four different sequences of RH exposure (60 s) (Table 1 and Fig. S4). The particles were subsequently further exposed to ammonia in a 6.6-L Erlenmeyer flask (400 s). Ammonia (0–15 cm^3 min^{-1}) was supplied from a standard cylinder (520.1 ppm; Airgas) and diluted by purified or humidified air (200 cm^3 min^{-1}). The humidified air was generated by bubbling purified air through water. The diluted ammonia flow was injected at the bottom of the flask using a T-shaped fitting to facilitate mixing (Fig. S4). The particle flow (800 cm^3 min^{-1}) was injected slightly above the ammonia injection port. Particles were sampled for further analysis from the top of the flask.

Changes upon ammonia exposure in the number–diameter distributions and the chemical composition of the particles were characterized using a SMPS and a high-resolution time-of-flight AMS. The particle flow passed through a diffusion dryer prior to the SMPS measurements. The AMS sampled the particle flow directly without a diffusion dryer. The AMS collection efficiency, which is defined here as primarily related to particle bounce, is also affected by uncertainties in the AMS ionization efficiency, the SMPS multiple charge correction, and any possible bias in particle sampling (Fig. S5).

ACKNOWLEDGMENTS. We thank R. Lebouteiller for contribution to the preliminary experiments and development of a new particle generator; Q. Chen for fruitful discussion on AMS data analysis; Y. Liu for measurement of the chemical composition of the purified air; and A. Bateman, M. L. Smith, G. Zhang, and S. R. Zorn for useful discussion and assistance with the experiments. This study was supported by the Office of Science (BES), US Department of Energy, Grant No. DE-FG02-08ER64529. M.K. was supported by a Japan Society for the Promotion of Science (JSPS) postdoctoral fellowship for research abroad.

1. Hallquist M, et al. (2009) The formation, properties and impact of secondary organic aerosol: Current and emerging issues. *Atmos Chem Phys* 9:5155–5236.
2. Pankow JF (1994) An absorption-model of gas-particle partitioning of organic-compounds in the atmosphere. *Atmos Environ* 28:185–188.
3. Odum JR, et al. (1996) Gas/particle partitioning and secondary organic aerosol yields. *Environ Sci Technol* 30:2580–2585.
4. Seinfeld JH, Pankow JF (2003) Organic atmospheric particulate material. *Annu Rev Phys Chem* 54:121–140.
5. Chan AWH, Kroll JH, Ng NL, Seinfeld JH (2007) Kinetic modeling of secondary organic aerosol formation: Effects of particle- and gas-phase reactions of semivolatile products. *Atmos Chem Phys* 7:4135–4147.
6. Chen Q, Liu YJ, Donahue NM, Shilling JE, Martin ST (2011) Particle-phase chemistry of secondary organic material: Modeled compared to measured O:C and H:C elemental ratios provide constraints. *Environ Sci Technol* 45:4763–4770.
7. Bahreini R, et al. (2005) Measurements of secondary organic aerosol from oxidation of cycloalkenes, terpenes, and m-xylene using an Aerodyne aerosol mass spectrometer. *Environ Sci Technol* 39:5674–5688.
8. Virtanen A, et al. (2010) An amorphous solid state of biogenic secondary organic aerosol particles. *Nature* 467:824–827.
9. Vaden TD, Imre D, Beranek J, Shrivastava M, Zelenyuk A (2011) Evaporation kinetics and phase of laboratory and ambient secondary organic aerosol. *Proc Natl Acad Sci USA* 108:2190–2195.
10. Perraud V, et al. (2012) Nonequilibrium atmospheric secondary organic aerosol formation and growth. *Proc Natl Acad Sci USA* 109:2836–2841.
11. Saukko E, et al. (2012) Humidity-dependent phase state of SOA particles from biogenic and anthropogenic precursors. *Atmos Chem Phys* 12:7517–7529.
12. Koop T, Bookhold J, Shiraiwa M, Poeschl U (2011) Glass transition and phase state of organic compounds: Dependency on molecular properties and implications for secondary organic aerosols in the atmosphere. *Phys Chem Chem Phys* 13:19238–19255.
13. Murray BJ (2008) Inhibition of ice crystallisation in highly viscous aqueous organic acid droplets. *Atmos Chem Phys* 8:5423–5433.
14. Mikhailov E, Vlasenko S, Martin ST, Koop T, Poschl U (2009) Amorphous and crystalline aerosol particles interacting with water vapor: Conceptual framework and experimental evidence for restructuring, phase transitions and kinetic limitations. *Atmos Chem Phys* 9:9491–9522.
15. Zobrist B, et al. (2011) Ultra-slow water diffusion in aqueous sucrose glasses. *Phys Chem Chem Phys* 13:3514–3526.
16. Shiraiwa M, Ammann M, Koop T, Poeschl U (2011) Gas uptake and chemical aging of semisolid organic aerosol particles. *Proc Natl Acad Sci USA* 108:11003–11008.
17. Hearn JD, Smith GD (2005) Measuring rates of reaction in supercooled organic particles with implications for atmospheric aerosol. *Phys Chem Chem Phys* 7:2549–2551.
18. Katrib Y, et al. (2005) Ozonolysis of mixed oleic-acid/stearic-acid particles: Reaction kinetics and chemical morphology. *J Phys Chem A* 109:10910–10919.
19. Huff Hartz KE, Weitkamp EA, Sage AM, Donahue NM, Robinson AL (2007) Laboratory measurements of the oxidation kinetics of organic aerosol mixtures using a relative rate constants approach. *J Geophys Res* 112:D04204.
20. Bilde M, Svenningsson B (2004) CCN activation of slightly soluble organics: The importance of small amounts of inorganic salt and particle phase. *Tellus B* 56:128–134.
21. Hartz KEH, et al. (2006) Cloud condensation nuclei activation of limited solubility organic aerosol. *Atmos Environ* 40:605–617.
22. Rissman TA, et al. (2007) Cloud condensation nucleus (CCN) behavior of organic aerosol particles generated by atomization of water and methanol solutions. *Atmos Chem Phys* 7:2949–2971.
23. Bouwman AF, et al. (1997) A global high-resolution emission inventory for ammonia. *Global Biogeochem Cycle* 11:561–587.
24. Kang SC, et al. (2002) Twentieth century increase of atmospheric ammonia recorded in Mount Everest ice core. *J Geophys Res* 107:4595.
25. Krupa SV (2003) Effects of atmospheric ammonia (NH_3) on terrestrial vegetation: A review. *Environ Pollut* 124:179–221.
26. George IJ, Abbatt JPD (2010) Chemical evolution of secondary organic aerosol from OH-initiated heterogeneous oxidation. *Atmos Chem Phys* 10:5551–5563.
27. Heald CL, et al. (2012) Atmospheric ammonia and particulate inorganic nitrogen over the United States. *Atmos Phys Chem Discuss* 12:19455–19498.
28. Wang SC, Flagan RC (1990) Scanning electrical mobility spectrometer. *Aerosol Sci Technol* 13:230–240.
29. DeCarlo PF, et al. (2006) Field-deployable, high-resolution, time-of-flight aerosol mass spectrometer. *Anal Chem* 78:8281–8289.
30. Allan JD, et al. (2004) A generalised method for the extraction of chemically resolved mass spectra from aerodyne aerosol mass spectrometer data. *J Aerosol Sci* 35:909–922.
31. Matthew BM, Middlebrook AM, Onasch TB (2008) Collection efficiencies in an Aerodyne Aerosol Mass Spectrometer as a function of particle phase for laboratory generated aerosols. *Aerosol Sci Technol* 42:884–898.
32. Hings SS, et al. (2008) CCN activation experiments with adipic acid: Effect of particle phase and adipic acid coatings on soluble and insoluble particles. *Atmos Chem Phys* 8:3735–3748.
33. Soonsin V, Zardini AA, Marcolli C, Zuend A, Krieger UK (2010) The vapor pressures and activities of dicarboxylic acids reconsidered: The impact of the physical state of the aerosol. *Atmos Chem Phys* 10:11753–11767.
34. Raymond TM, Pandis SN (2002) Cloud activation of single-component organic aerosol particles. *J Geophys Res* 107:4787.
35. Chan MN, Kreidenweis SM, Chan CK (2008) Measurements of the hygroscopic and deliquescence properties of organic compounds of different solubilities in water and their relationship with cloud condensation nuclei activities. *Environ Sci Technol* 42:3602–3608.
36. Mircea M, et al. (2005) Importance of the organic aerosol fraction for modeling aerosol hygroscopic growth and activation: A case study in the Amazon Basin. *Atmos Chem Phys* 5:3111–3126.
37. Biskos G, Malinowski A, Russell LM, Buseck PR, Martin ST (2006) Nanosize effect on the deliquescence and the efflorescence of sodium chloride particles. *Aerosol Sci Technol* 40:97–106.
38. Varutbangkul V, et al. (2006) Hygroscopicity of secondary organic aerosols formed by oxidation of cycloalkenes, monoterpenes, sesquiterpenes, and related compounds. *Atmos Chem Phys* 6:2367–2388.
39. Smith ML, Kuwata M, Martin ST (2011) Secondary organic material produced by the dark ozonolysis of alpha-pinene minimally affects the deliquescence and efflorescence of ammonium sulfate. *Aerosol Sci Technol* 45:244–261.
40. Pankow JF (2010) Organic particulate material levels in the atmosphere: Conditions favoring sensitivity to varying relative humidity and temperature. *Proc Natl Acad Sci USA* 107:6682–6686.
41. Zuend A, Seinfeld JH (2012) Modeling the gas-particle partitioning of secondary organic aerosol: The importance of liquid-liquid phase separation. *Atmos Chem Phys* 12:3857–3882.
42. Shilling JE, et al. (2008) Particle mass yield in secondary organic aerosol formed by the dark ozonolysis of alpha-pinene. *Atmos Chem Phys* 8:2073–2088.
43. Kuwata M, Chen Q, Martin ST (2011) Cloud condensation nuclei (CCN) activity and oxygen-to-carbon elemental ratios following thermodenuder treatment of organic particles grown by α-pinene ozonolysis. *Phys Chem Chem Phys* 13:14571–14583.
44. Na K, Song C, Switzer C, Cocker DR, III (2007) Effect of ammonia on secondary organic aerosol formation from alpha-pinene ozonolysis in dry and humid conditions. *Environ Sci Technol* 41:6096–6102.
45. Jimenez JL, et al. (2003) Ambient aerosol sampling using the Aerodyne Aerosol Mass Spectrometer. *J Geophys Res* 108:8425.
46. Malloy QGJ, et al. (2009) Secondary organic aerosol formation from primary aliphatic amines with NO_3 radical. *Atmos Chem Phys* 9:2051–2060.
47. Laskin J, et al. (2010) High-resolution desorption electrospray ionization mass spectrometry for chemical characterization of organic aerosols. *Anal Chem* 82:2048–2058.
48. Chen Q, Liu Y, Donahue NM, Shilling JE, Martin ST (2011) Measured O:C and H:C elemental ratios constrain the production mechanisms of biogenic secondary organic material. *Environ Sci Technol* 45:4763–4770.